

# Molecular Spin-Flip Loss and a Dual Quadrupole Trap

David Reens,<sup>\*</sup> Hao Wu, Tim Langen,<sup>†</sup> and Jun Ye

*JILA, National Institute of Standards and Technology and the University of Colorado  
Department of Physics, University of Colorado, Boulder, Colorado 80309-0440, USA*

(Dated: April 17, 2017)

EDIT ME LATER. A new electromagnetic trap geometry allows full tuning of complex molecular spin-dynamics in crossed electric and magnetic fields. If not tuned properly, these dynamics lead to spin-flip loss that afflicts a wide set of candidate molecules. The spin-flip loss can be significant even above 100 mK and varies inversely with temperature, so it's removal represents a critical step toward ultracold molecules. The trapping geometry features a 0.5 K trap depth and 5 T/cm trap strength, and allows spin-dynamics to be tuned with a weak external bias coil. Spin-flip loss is tuned in a 170 mK sample of OH molecules from over  $200 \text{ s}^{-1}$  to below the vacuum limited lifetime of  $2 \text{ s}^{-1}$ .

The ultracold regime extends toward molecules on many fronts [1]. Several alkali molecules are available [2–4] and others are under development. Creative and carefully engineered laser cooling strategies are tackling certain nearly vibrationally diagonal molecules [5–9]. A diverse array of alternative strategies have succeeded to greater or lesser extents on other molecules [10–14]. All of these molecules will require secondary strategies like evaporation or sympathetic cooling to make further gains in phase space density. They also may face a familiar challenge: spin flip loss near the zero of a magnetic trap, but dramatically enhanced for many doubly dipolar molecules due to their internal spin dynamics in mixed electric and magnetic fields.

The knowledge of spin flips or Majorana hops as an eventual trap lifetime limit predates the very first magnetic trapping of neutrals [15]. Spin flips were directly observed near  $10 \mu\text{K}$  and overcome in the TOP trap [16], and soon later with a plugged dipole trap [17], famously enabling the first Bose-Einstein condensates. In our earlier investigations, we observed OH trap loss with applied electric field [? ]. This trap loss occurred for sub-states of OH's  $X^2\Pi_{3/2}$  ground state manifold other than the most well-trapped one, and was attributable to avoided crossings that open at non-zero magnetic fields between levels of opposite parity. We have now identified trap loss at zero magnetic field with the application of electric field that afflicts even the most well-trapped substate although it lacks any crossings with opposite parity states.

We observe spin-flips in a Stark-decelerated OH sample, about four orders of magnitude higher in temperature compared with the atomic case. In our new dual quadrupole trap, it is possible to tune this loss over a wide dynamic range, but we begin with our previous geometry [18], a 3D permanent magnet quadrupole trap with homogeneous electric field applied, as our starting point to explain the internal spin-dynamics that lead to the spin-flip loss. As will be seen, the internal spin-dynamics are applicable to all Hund's case (a) states and also to Hund's case (b) states to a lesser extent.

The internal spin-dynamics that lead to this enhanced

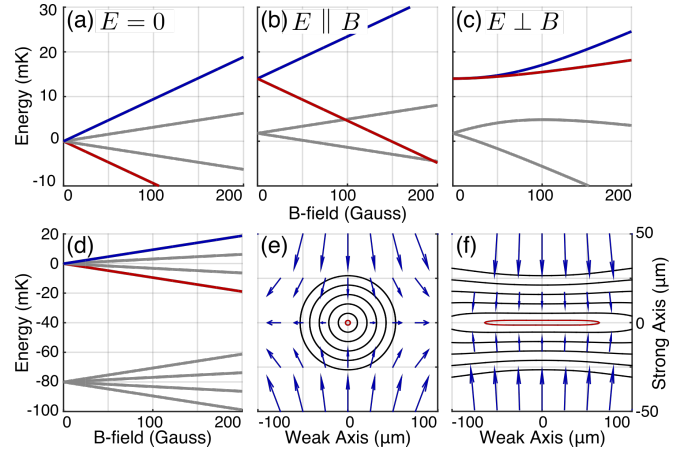


FIG. 1. The blocking effect. (a), four Zeeman split lines in OH's  $J = 3/2$  ground manifold. An opposite parity manifold sits 100 mK below. The trapped state (blue) and its spin-flip partner (red). (b) Zeeman splitting,  $E \parallel B$ ,  $E = 150 \text{ V/cm}$ . (c)  $E \perp B$ . Note vastly reduced red-blue splitting. See other angles in appendix of [19]. (d) Energy splitting contours every 2 mK near the zero of our 2 T/cm trap [20]. B-field arrows in blue. (e) Again with  $E = 150 \text{ V/cm}$ . Note drastic widening of lowest contour (red). Vector direction gives the Hund's Case X quantization axis of trapped state,  $\mu_B B \pm d_E E$  above (below) the center plane. Vector magnitude gives potential energy relative to trap center.

spin-flip loss are subtle; it has taken a concentrated several year effort to elucidate the effect with conclusive experimental evidence as reported here. These internal spin-dynamics have also eluded three previous investigations of note: In [21] the analogues of atomic spin-flip loss for molecules in mixed fields were investigated, and a magnetic quadrupole trap for OH molecules with superposed electric field was specifically addressed. It was concluded that no significant loss enhancement due to electric field should be evident. While this is true for the approximate  $^2\Pi_{1/2}$  Hamiltonian used in that study, it is not true for the actual  $^2\Pi_{3/2}$  ground state of OH. In [19] E-fields were applied in our magnetic quadrupole trap to study E-field induced collisions. Although an ini-

tial awareness existed of the effect we describe, efforts to deconvolve it underestimated the magnitude of the spin-flip loss. [22] Finally, in [23] it was correctly noted that Hund's case (a) molecules maintain a quantization axis in mixed fields. In fact the states of the molecule align with one of two quantization axes- either the vector sum or the vector difference of the dipole moment weighted electric and magnetic fields. It was asserted that this would maintain quantization near the zero of a quadrupole trap and avoid spin-flip loss. As we will now explain, quantization is indeed maintained, but spin-flip loss is enhanced:

With only magnetic field, a molecule remains trapped insofar as it adiabatically follows the field direction. Near the trap center, the direction changes most rapidly, enabling loss. When electric field is added, it dominates in the trap center where the magnetic field is weakest. Quantization is maintained but the quantization axis does not rotate with the magnetic field as it needs to. Further away from the trap center the molecule is then magnetically strong field seeking and is lost. The molecule ought to have switched from the vector sum quantization axis to the vector difference quantization axis, so as to remain doubly weak field seeking despite the change in relative orientation of the fields. To be more precise, we define the relative orientation of the fields as the sign of  $\phi = E \cdot B$ . When  $\phi$  is negative (positive), the doubly trapped state must have the vector difference (sum) quantization axis, so that an increase in magnitude of either field increases its energy. Orientation changes whenever  $\phi$  changes sign, which occurs in a 2D region given by  $\phi = 0$ , i.e.  $E \perp B$ . This region must by 2D, since it is a contour level of the 3D scalar valued function  $\phi$ .

We can also understand this effect in terms of the energy splitting between the well trapped substate and its spin-flip partner, since this splitting acts as a barrier to spin-flips. The preceding quantization axis discussion suggests that spin-flips can occur in the  $\phi = 0$  planar region, so we expect to find a correspondingly reduced energy splitting there. In Fig. 1, the energies of the well trapped state and its spin-flip partner are calculated by diagonalizing OH's  $X^2\Pi_{3/2}$  ground state Hamiltonian verses B-field without E-field in panel (a), with fixed E-field and  $E \parallel B$  so that  $\phi$  is maximally nonzero in panel (b), and with fixed E-field and  $\phi = 0$  in panel (c). Indeed, we find a striking reduction in energy splitting for a wide range of magnetic fields in panel (c) compared with panel (b). In fact, by series expanding the exact eigenenergies of OH, we find  $H_{E \perp B}(B) \approx (\mu_B B)^3 \Delta^2 / (d_E E)^4$ ,  $\Delta$  the lambda doubling term. The Zeeman splitting is no longer linear, but cubic. This means that the splitting will be small in a much larger region close to  $B = 0$  than otherwise.

This observation allows us to develop a scaling law for the loss enhancement in the magnetic quadrupole with

TABLE I. Enhancements and loss rates for OH. Evaporation E-field detailed in [25]. Spectroscopic E-field in [20]. Background loss is  $2 \text{ s}^{-1}$ , experiment length 100 ms.

$E \text{ (V/cm)}$	45 mK		5 mK		Purpose
	$\nu$	$\Gamma \text{ (s}^{-1}\text{)}$	$\nu$	$\Gamma \text{ (s}^{-1}\text{)}$	
0	1	0.02	1	1.3	No Field
300	5	0.1	9	11	Evaporation
550	17	0.3	40	50	Spectroscopy
3000	1000	19	1600	2000	Polarizing

superposed electric field case. For a given trap strength and sample temperature, there is a characteristic energy splitting  $\kappa$  below which spin-flips can occur, calculated from the Landau-Zener formula. In our case  $\kappa = 5 \text{ MHz}$ . As shown in panel (e) of fig. 1, E-field widens the  $\kappa$  valued energy contour near the trap zero, greatly increasing the flux through this region. Note also that the energy gradient near the loss region, which also contributes to the Landau-Zener hopping probability, remains nearly identical in the z-direction between panels (d) and (e). Solving for  $B$  when  $H_{E \perp B}(B) = \kappa$  and dividing by the  $E = 0$  case gives the flux enhancement factor  $\nu = (d_E E / \sqrt{\kappa \Delta})^{8/3}$ . So E-fields beyond  $\sqrt{\kappa \Delta}$  lead to almost cubic enhancements in spin-flip loss. We can be more quantitative by integrating the velocity distribution and the flux through the plane, accounting for the velocity dependent Landau-Zener probability, Table. I. The spin-flip loss is negligible at 50 mK, but relevant at the 5 mK targeted during evaporation [25]. Those results will thus require reinterpretation considering this effect [26]. With the goal of  $\mu\text{K}$  temperatures and below, it is clear spin-flip loss must be addressed.

For Hund's case (a) states more generally, the Zeeman splitting when  $E \perp B$  is reduced from linear to order  $2J$ , according to several test Hamiltonians we have diagonalized. This also agrees with the intuition that when  $\mu_B B \ll d_E E$  and  $E \perp B$ , the magnetic field must undo the electric field's coupling of opposite  $m_J$  number states, a task of order  $m_J - -m_J = 2J$ . Thus only  $J = 1/2$  states are immune, but these are not magnetically trappable due to their vanishing g-factor anyway. For Hund's case (b) the enhanced loss region is restricted to the trap energy regime where  $\gamma$  the spin-rotation coupling dominates. In this region the state is effectively Hund's case (a). This can still be very significant, for example  $\gamma = 75 \text{ MHz}$  for SrF [24]. In preliminary investigations for Hund's case (b) molecules, which essentially consist of reproducing panels (a)-(c) of Fig. 1 for different Hamiltonians, we find large spin-flip loss enhancements for SrF's  $v=0$ ,  $N=1$  magnetically trappable substates. Some Hund's case (b) molecular states such as YO's  $v=0$ ,  $N=1$  manifold have a protected substate with  $m_F = 0$  and thus no hopping partner in the spin-rotation coupling regime that is nonetheless energetically separated

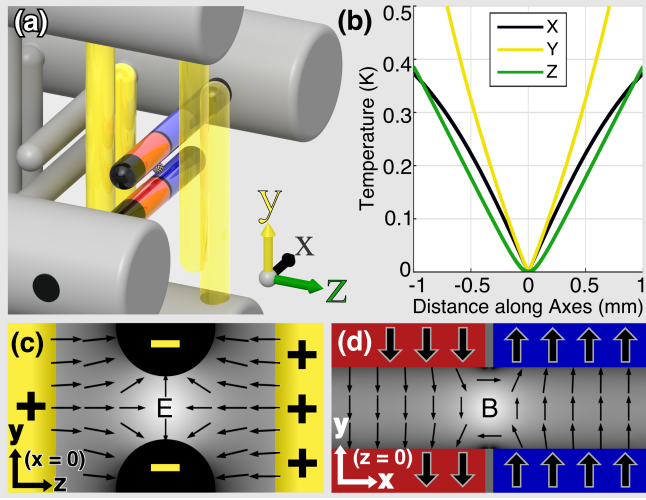


FIG. 2. Dual quadrupole trap embedded in Stark Decelerator. (a) The decelerator has four backbone electrodes (red) and many pin electrodes (gray). OH produced and slowed as in [18], except the slowing extends nearly to zero velocity between the second to last pin pair (black), magnetized as in (c). Four pins form the electric trapping quadrupole (yellow, one omitted for clarity), the last and third to last pin pairs. Detail in (b). Trapping pins are conductive with decelerator backbone; voltage configurations achieved with existing feedthroughs but modified MOSFET setup for bipolar output. Yellow bidirectional arrows indicate translation described in text. Bias coils (light blue) sit outside vacuum. LIF detection with laser (pink) and collection lens (blue). (d), trap energy along axes.  $B' = 5$  T/cm and  $E' = 100$  kV/cm<sup>2</sup>. Trap frequencies  $\nu_x = 3$  kHz,  $\nu_y = 5$  kHz, and  $\nu_z = 4$  kHz.

from other state-crossings by the lamb-shift. This state is less strongly trappable due to the same  $m_F = 0$  feature, but is fully spin-flip immune even in a magnetic quadrupole trap with superposed electric field.

We can generalize to arbitrary geometries with a simple strategy: avoid  $\mu_B B < d_E E$  where  $E \perp B$ . One way to achieve this is to trap with E-field and superpose B-field. The lambda doublet prevents flips in this configuration, but it does round the trap considerably near the center. Another option is to trap with both fields and keep zeros overlapped. This was once realized for OH with a superposed magnetic quadrupole and electric hexapole [27]. Such a scheme prevents spin-flip loss enhancement, but does not remove it entirely. It is also susceptible to misalignment induced spin-flip loss. A final possibility is the use of only a single field. While this avoids spin-flip loss enhancement, any experiment which aims to make use of the doubly dipolar nature of molecules cannot accept this compromise.

Seeking to remove the loss entirely but without sacrificing trap depth or gradient, we use a pair of 2D quadrupole traps, one magnetic and the other electric, with orthogonal axes. We achieve these fields with a ge-

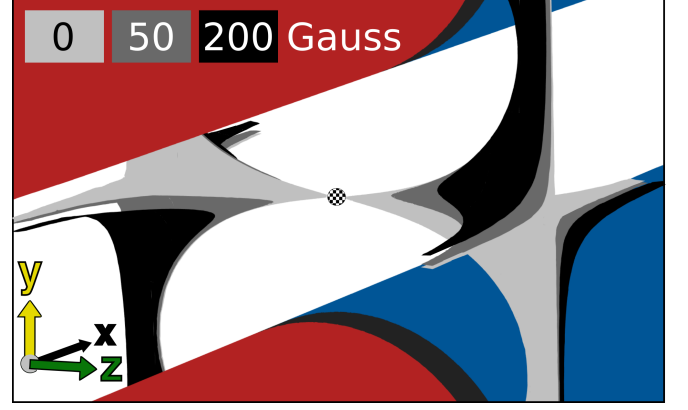


FIG. 3. Surfaces where spin-flips can occur for several values of  $B_{\text{coil}}$ . Trap energy contours every 100 mK (gray).  $B_{\text{coil}}$  pushes loss regions away from the trap center.

ometry that matches our Stark decelerator [13], as shown in Fig. 2. This approach is similar to the Ioffe-Pritchard strategy [28], where a 2D quadrupole is combined with an axial dipole trap. Axial and radial trapping interfere, resulting in significantly lower trap depths than the 3D quadrupole. We thwart this interference by using electric field for the third direction. This geometry has  $E \perp B$  along both the  $xz$  and  $yz$  planes, with  $\mu_B B < d_E E$  in a large cylinder surrounding the  $z$ -axis. However, by adding magnetic field along the zero axis of the magnetic quadrupole with external bias coils, a fully tunable scenario emerges.

$B_{\text{coil}}$  allows a full tuning from  $200 \text{ s}^{-1}$  to complete removal, see Fig. 4, panel (a). It does this by morphing the  $E \perp B$  surface from a pair of planes into a hyperbolic sheet which deviates spatially from the magnetic field minimum along the  $z$ -axis. Thanks to this deviation, for suitable magnitude of  $B_{\text{coil}}$ ,  $\mu_B B < d_E E$  can be avoided. In fig. 3, the surfaces where  $E \perp B$  are colored wherever the splitting there is below the hopping threshold  $\kappa$ . Note how  $B_{\text{coil}}$  tunes the proximity of the loss regions to zero. The loss regions are always visible, but they are tuned so far from the trap center that molecules accessing them have already escaped the trap.

As a further confirmation of our  $E \perp B$  and  $\mu_B B < d_E E$  model of the loss, we translate our magnetic pins in their mounts to alter the surface where  $E \perp B$  and compare experimental data against our expectations. The data are shown in fig. 4. Qualitatively, this translation serves to disrupt the otherwise perfectly 2D magnetic quadrupole by adding a small trapping field  $\vec{B} \propto B' z \hat{z}$  along the  $z$ -axis. This means that  $B_{\text{coil}}$  no longer directly tunes the minimum magnetic field in the trap. Instead,  $B_{\text{coil}}$  must first overcome the slight trapping field along the  $z$ -axis, translating a point of zero field along the  $z$  axis and eventually out of the trap. The point of zero field disrupts the previously hyperbolic  $E \perp B$  surface, causing it to twist and intersect the  $z$ -axis near the mag-

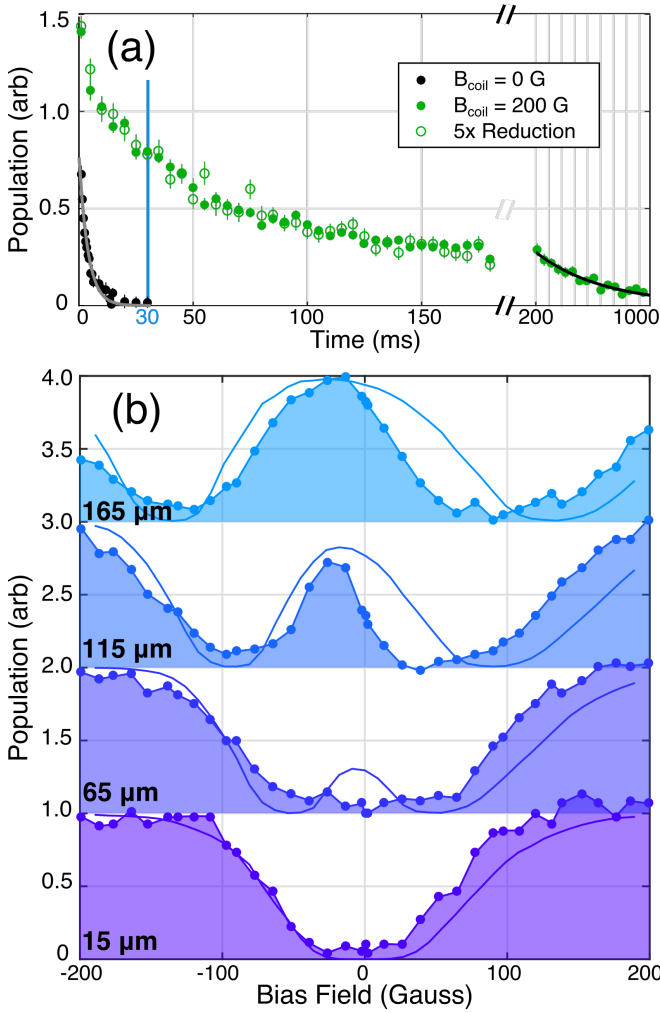


FIG. 4. (a) Time traces for aligned pins at two bias fields, a density modulated trace, and an extended time trace. (b) At the fixed time 30ms, population as a function of pin translation and bias field.

netic zero. This intersection point has  $\mu_B B \ll d_E E$  except when aligned with the trap center, where  $E$  also goes to zero. This means that without any bias field, the loss should actually be a local minimum; as the field is increased in either direction the loss should first worsen and then improve when the zero leaves the trap. This qualitative explanation correctly predicts the observed double well structure.

Quantitatively, we fit the family of curves shown in fig. 4 by performing an integration of molecule flux weighted by Landau-Zener probability and Maxwell-Boltzmann population density over the strangely twisted hyperbola of  $E \perp B$ . The computation is performed in COMSOL Multiphysics, accounting for the expected magnetic and electric fields from the trapping geometry with various offsets and with cloud temperature as the only free parameter [29]. The fit temperature is approximately 170 mK. The asymmetry of the curves about the

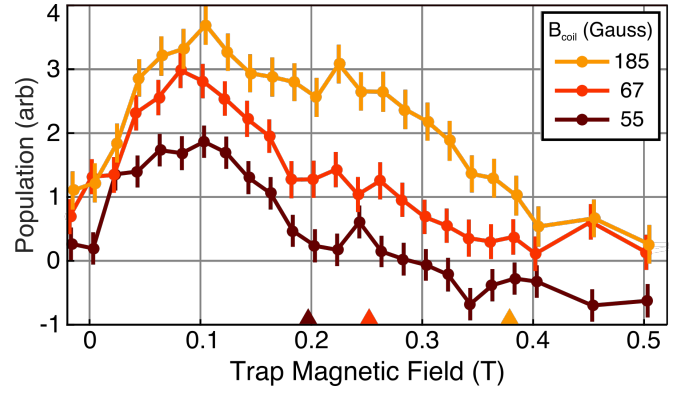


FIG. 5. Microwave Thermometry. Bias field tunes the proximity of loss to the trap center.

$B_{\text{coil}} = 0$  axis comes from a slight shift of the electric quadrupole minimum caused by an intentional bending of the last pin pair to increase fluorescence collection. This offset is not a free parameter in the model, it is directly included according to the measured bending applied to the pins. The fitted temperature is larger than expected from our simulations of the geometry, despite the known defocusing and reflection losses that accompany pulsed decelerators at low speeds [30]. This may be related to micro-discharges on the surfaces of the magnetic pins during the final deceleration pulse. The magnetic pins are not currently polished as well as the rest of the decelerator, but this is not a fundamental limitation and could be overcome by diamond turning of the nickel plating on the pins or some other polishing strategy.

Another way to validate our understanding of molecular spin-flip loss in our dual quadrupole trap would be to confirm that the location of the loss is indeed pushed away from the trap center with increasing  $B_{\text{coil}}$  as shown in fig. 3. We achieve this with a Zeeman microwave spectroscopy performed as in our previous work [25]. Rather than using a bias tee setup, we use a microwave probe to directly excite free space cavity modes of our vacuum chamber. The results are shown in fig. 5. With the magnetic pins aligned, it is seen that higher values of  $B_{\text{coil}}$  indeed increases the population of molecules able to survive at higher fields. In order to perform this spectroscopy, the trapping electric fields are switched off immediately prior to the application of a microwave transfer pulse tuned to a particular magnetic field strength. Thus the results reflect the Zeeman potential energy only, and only loosely correspond to the total potential energy of the molecules. Nonetheless, the shift in population center is clear and in agreement with our expectation.

In the case of lowest applied magnetic field in fig. 5, i.e. deepest cutting of the loss region toward the trap center, a negative going signal is observed. This indicates a build-up in the opposite parity weak electric field seeking state. Although the spin-flips we have discussed

connect strong and weak field seeking magnetic states, other avoided crossings amongst the ground state manifold result in the spin-flipped molecules remaining very weakly trapped in a secondary state with opposite parity character in some regions.

Once the loss is fully removed, we observe the trend in panel (a) of fig. 4. The decay rate decreases with population over a timescale that is long compared with trap frequency and is thus suggestive of a collisional process. However, a completely phase-space blind density reduction technique [31] that significantly reduces our molecule number causes little change in the trend, indicating that single-particle physics is responsible. This is attributable to our warmer initial temperature than in previous experiments. The slowly decaying trend could be related to the existence of high energy chaotic orbits with long escape times, as seen in other exotically shaped trapping potentials [32]. We hope in the near future to implement several molecule number enhancement strategies.

Our dual quadrupole trap decisively overcomes molecule enhanced spin-flip loss by tuning it from an overwhelming rate to complete removal. Our explanation of the loss provides detailed predictions of how its location and magnitude ought to scale with bias field and trap alignment, which we have experimentally verified. Our results contradict existing predictions about molecular spin-flips in mixed fields and we provide a consistent framework that explains this based on internal spin-dynamics. We have devised a viable trapping geometry in which spin-flip loss is fully mitigated without trap-depth sacrifice, paving the way toward further improvements in molecule trapping and cooling.

We acknowledge our the Gordon and Betty Moore Foundation and the AFOSR for their financial support. T.L. acknowledges support by the Alexander von Humboldt Foundation through a Feodor Lynen Fellowship. We thank J.L. Bohn and S.Y.T. van de Meerakker for helpful discussions.

D.R. and H.W. contributed equally to this work: D.R. in writing and trap design, H.W. in experiment execution.

---

\* dave.reens@colorado.edu

† Present Address: 5. Physikalisches Institut and Center for Integrated Quantum Science and Technology (IQST), Universität Stuttgart, Pfaffenwaldring 57, 70569 Stuttgart, Germany

- [1] L. D. Carr, D. DeMille, R. V. Krems, and J. Ye, *New Journal of Physics* **11**, 055049 (2009).
- [2] K.-K. Ni, S. Ospelkaus, M. H. G. de Miranda, A. Pe'er, B. Neyenhuis, J. J. Zirbel, S. Kotochigova, P. S. Julienne, D. S. Jin, and J. Ye, *Science* **322**, 231 (2008).
- [3] T. Takekoshi, L. Reichsöllner, A. Schindewolf, J. M. Hutson, C. R. Le Sueur, O. Dulieu, F. Ferlaino, R. Grimm, and H.-C. Nägerl, *Physical Review Letters* **113**, 205301 (2014).
- [4] J. W. Park, S. A. Will, and M. W. Zwierlein, *Physical Review Letters* **114**, 205302 (2015).
- [5] M. H. Steinecker, D. J. McCarron, Y. Zhu, and D. DeMille, *ChemPhysChem* **17**, 3664 (2016).
- [6] J. F. Barry, D. J. McCarron, E. B. Norrgard, M. H. Steinecker, and D. DeMille, *Nature* **512**, 286 (2014).
- [7] B. Hemmerling, E. Chae, A. Ravi, L. Anderegg, G. K. Drayna, N. R. Hutzler, A. L. Collopy, J. Ye, W. Ketterle, and J. M. Doyle, *Journal of Physics B: Atomic, Molecular and Optical Physics* **49**, 174001 (2016).
- [8] M. T. Hummon, M. Yeo, B. K. Stuhl, A. L. Collopy, Y. Xia, and J. Ye, *Physical Review Letters* **110**, 143001 (2013).
- [9] V. Zhelyazkova, A. Cournol, T. E. Wall, A. Matsushima, J. J. Hudson, E. A. Hinds, M. R. Tarbutt, and B. E. Sauer, *Physical Review A* **89**, 053416 (2014).
- [10] J. M. Doyle, J. D. Weinstein, R. DeCarvalho, T. Guillet, and B. Friedrich, *Nature* **395**, 148 (1998).
- [11] A. Prehn, M. Ibrügger, R. Glöckner, G. Rempe, and M. Zeppenfeld, *Physical Review Letters* **116**, 063005 (2016).
- [12] H. L. Bethlem, G. Berden, and G. Meijer, *Physical Review Letters* **83**, 1558 (1999).
- [13] J. R. Bochinski, E. R. Hudson, H. J. Lewandowski, G. Meijer, and J. Ye, *Physical Review Letters* **91**, 243001 (2003).
- [14] N. Akerman, M. Karpov, L. David, E. Lavert-Ofir, J. Narevicius, and E. Narevicius, *New Journal of Physics* **17**, 065015 (2015).
- [15] A. L. Migdall, J. V. Prodan, W. D. Phillips, T. H. Bergeman, and H. J. Metcalf, *Physical Review Letters* **54**, 2596 (1985).
- [16] W. Petrich, M. H. Anderson, J. R. Ensher, and E. A. Cornell, *Physical Review Letters* **74**, 3352 (1995).
- [17] K. B. Davis, M. O. Mewes, M. R. Andrews, N. J. van Druten, D. S. Durfee, D. M. Kurn, and W. Ketterle, *Physical Review Letters* **75**, 3969 (1995).
- [18] B. C. Sawyer, B. K. Stuhl, D. Wang, M. Yeo, and J. Ye, *Physical Review Letters* **101**, 203203 (2008).
- [19] B. K. Stuhl, M. Yeo, M. T. Hummon, and J. Ye, *Molecular Physics* **111**, 1798 (2013).
- [20] B. K. Stuhl, M. Yeo, B. C. Sawyer, M. T. Hummon, and J. Ye, *Physical Review A* **85**, 033427 (2012).
- [21] M. Lara, B. L. Lev, and J. L. Bohn, *Physical Review A* **78**, 033433 (2008).
- [22] It is unclear how much of the collisional effect described in [19] remains. This will be the subject of further investigation.
- [23] J. L. Bohn and G. Quémener, *Molecular Physics* **111**, 1931 (2013).
- [24] G. Quémener and J. L. Bohn, *Physical Review A - Atomic, Molecular, and Optical Physics* **93**, 1 (2016).
- [25] B. K. Stuhl, M. T. Hummon, M. Yeo, G. Quémener, J. L. Bohn, and J. Ye, *Nature* **492**, 396 (2012).
- [26] Spin-flip loss would have interfered with evaporation before 5 mK was attained. Some phase space compression does seem to have occurred at 20 mK.
- [27] B. C. Sawyer, B. L. Lev, E. R. Hudson, B. K. Stuhl, M. Lara, J. L. Bohn, and J. Ye, *Physical Review Letters* **98**, 1 (2007).
- [28] D. E. Pritchard, *Physical Review Letters* **51**, 1336 (1983).
- [29] Source code: <https://github.com/dreens/spin-flip>

integration/.

- [30] B. C. Sawyer, B. K. Stuhl, B. L. Lev, J. Ye, and E. R. Hudson, *European Physical Journal D* **48**, 197 (2008).
- [31] Microwaves applied via our free space cavity mode probe couple electrically weak and strong field seeking states during first half of deceleration. Any spatial inhomogeneity in the microwaves, unlikely given the 15 cm wavelength, is sufficiently remixed during remaining deceleration and trap loading.
- [32] R. González-Férez, M. Iñarrea, J. P. Salas, and P. Schmelcher, *Physical Review E* **90**, 062919 (2014).